

Data Augmentation of Pseudo-Dense Images to Detect Morning Glory Regions in Soybean Fields

Aoi Kodama¹, Satoki Tsuichihara¹, and Yasutake Takahashi¹

Abstract—Morning glories prevent soybean growth and reduce yields. However, early morning glories are small and difficult to detect visually in the vast fields. Semantic segmentation effectively estimates the location of weeds using images captured by drones, but a large amount of image data is required to ensure high prediction accuracy, and an open dataset of plants with a wide variety of species is limited. In this research, we propose an image generation system of pseudo-dense morning glory using PGGAN to increase the volume of the dataset for training. The proposed pseudo images can configure the density of multiple morning glory using the distance. As a result of including these pseudo-densely morning glories, the F_2 score of the estimation was 0.404.

I. INTRODUCTION

In recent years, the decline in the number of agricultural workers and the aging population have made it difficult to manually control weeds across large fields. Therefore, the use of drones, which can automatically capture images of entire fields and move over large areas in a short time. Combined with machine-learning techniques, it is expected to reduce both time and monetary costs, facilitating more efficient weed management through data-driven smart agriculture [1].

In research [2][3][4] focused on fields have been carried out weed detection using machine learning with images captured by drones. Osorio Kavir et al. [2] investigated three weed estimation methods based on deep learning image processing (SVM with histograms of oriented gradients (HOG), YOLO-V3 and mask R-CNN) in lettuce crops using images captured by drones and compared to visual estimation by experts. The F_1 scores were 88%, 94% and 94% respectively. J. Rasmussen et al. [3] detected thistles in wheat and barley fields by classifying crops and thistles based on the excess green index (ExG) using orthomosaic images of entire fields generated from UAV images. They employed a semi-automatic program to determine thresholds, using two methods: manual adjustment based on visual threshold settings and threshold estimation based on annotated training data. They achieved weed detection accuracy exceeding 90%.

Research [4][5] has been carried out weed detection at the pixel level using semantic segmentation. W. Ramirez et al. [4] implemented a model to segment weeds in sugar beet farms using the DeepLabv3 architecture trained on

This work was partially supported by Research Grants from the University of Fukui (FY 2024).

¹Aoi Kodama, Satoki Tsuichihara, and Yasutake Takahashi are with the Department of Human and Artificial Intelligent Systems, University of Fukui, 3-9-1, Bunkyo, Fukui-shi, Fukui, 910-8507, Japan kodama.aoi@ir.his.u-fukui.ac.jp, satoki-t@u-fukui.ac.jp

patches extracted from high-resolution aerial images, achieving up to 0.89 and 0.81 in terms of AUC and F_1 scores, respectively. Kamath Radhika et al. [5] used three semantic segmentation models, including SegNet, PSPNet and UNet, were used for the segmentation of paddy crops and two weed species (sedges and broadleaved weeds), with promising results of over 90% accuracy. It shows that Deep Learning-based semantic segmentation of paddy crops and weeds can be used for sustainable site-specific weed management, leading to safe food production.

In soybean fields targeted in this research, naturalised morning glories such as Red morning glory and Ipomoea lacunosa have been found to invade soybean fields and have become a problem as difficult weeds to control in soybean fields [6]. Weeds are reported to reduce soybean yield by 50-60% [7] if weeds are unchecked, so early detection and control of weeds is one of the most important tasks.

Machine learning is used to estimate the location of weeds, but a large amount of image data is required to ensure high prediction accuracy. Research [8][9][10] has been carried out to increase detection accuracy by adding GAN [11]-generated images to the dataset in order to expand the dataset. LG Divyanth et al. [8] generated artificial images of corn and four types of weeds using conditional generative adversarial networks (cGAN) and added them to the dataset, which increased the F_1 score from 0.97 to 0.99. Borja Espejo-Garcia et al. [9] evaluated several architectures and configurations on a dataset containing tomato and black nightshade images. The best configuration was a combination of GAN and Xception network, which showed 99.07% performance.

In this research, data collection was conducted by capturing soybean fields with a drone, and images of early-stage

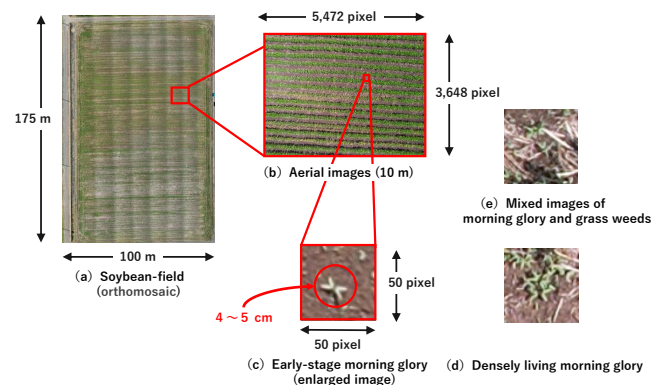


Fig. 1: Aerial images of soybean field and cropped images of morning glory

morning glories between the rows were used as training data. The target soybean field is shown in Fig. 1 (a), the aerial image captured by drone is shown in Fig. 1 (b), the morning glory images used for training are shown in Fig. 1 (c), the dense morning glory images are shown in Fig. 1 (d), and the mixed images of morning glory and grass weeds are shown in Fig. 1 (e). We prepared a training dataset of early-stage morning glories using the method by Sumi et al. [12], but the morning glories between the rows cannot be extracted completely. By using SegNet and training with only the morning glory data shown in Fig. 1 (c) as training images, we were able to detect morning glories between the rows. However, since most images depict single morning glories, it becomes difficult to detect regions where morning glories are densely clustered, as shown in Fig. 1 (d), or regions where morning glories mixed with grass weeds, as shown in Fig. 1 (e).

The objective of this research is to detect small morning glory, including mixed and complex areas around the rows of soybeans, using pseudo images. We build a system to generate pseudo images of morning glory with PGGAN and place the generated image into actual images of other weed to create artificially dense-mixed images of grass weed and morning glory for increasing the dataset.

II. GENERATION OF TRAINING DATA AND DEEP LEARNING FOR WEED DETECTION

Based on morning glory's living in the colony, we generate morning glory images using PGGAN. The generated images contain pseudo-dense images of morning glory. By adding the generated images to the dataset, the trained model estimates regions of the micro-morning glory using SegNet.

A. Generating Pseudo-Dense Images of Morning Glory

1) *PGGAN*: PGGAN [13] is a method in which training starts with low-resolution image generation, and as training progresses, higher-resolution convolution and transposed convolution layers are added to the generators and discriminators, respectively, and the resolution of the generated images is increased step by step.

2) *Selecting background images of the grass weed*: For adding the images of morning glory, we prepare background images containing other plants in the soybeans field. In this paper, the other plants are grass weed and soil.

I. Image Cropping

- Original aerial images (Fig. 1 (b)) captured by drones are cropped to 50×50 pixels.

II. Grass Weed Detection

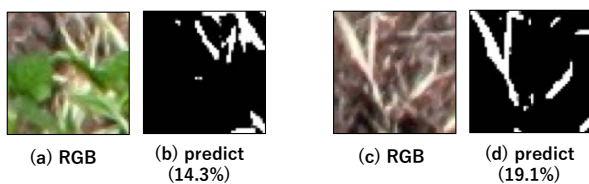


Fig. 2: Results of grass weed detection using SegNet

- The obtained images include four main types: soybean, morning glory, grass weeds, and soil.
- Figure 2 shows the input images (a) and (c) and the detection results (b) and (d) (white: grass weed). To obtain label images of grass weeds, the grass-weed model is trained using Segnet using 400 grass weed images through manual annotation to perform a two-class classification between grass weeds and others. The trained grass-weed model is used to detect grass-weed regions.

III. Selecting Images

- Based on the number of the pixels detected as the grass weed (Fig 2 (b) and (d)), images containing 10-20 % white pixels in each image are selected.

$$ExG = 2G - R - B \quad (1)$$

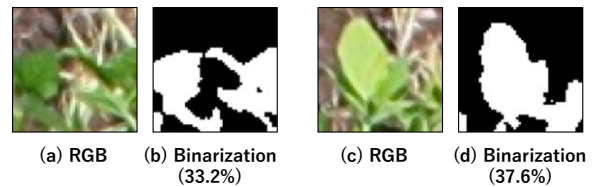


Fig. 3: Binaryisation of soybean areas using ExG index

- Figure 3 shows the selected images (a, c) and binary images using ExG index [14]. Equation 1 calculates ExG value using RGB values in the image. To remove images that contain large soybean leaves, we calculate ExG in the RGB images to classify the green areas. Binarization was implemented with ExG values of 1 for pixels with an ExG value of 130 or more and 0 for pixels with an ExG value of less than 130. Exclude images with white areas of more than 20%.

3) *Placing Pseudo-Dense Images of Morning Glory to Background Images without Overlapping*: We calculate coordinates to place the pseudo-dense images of the morning glory, which do not overlap with the grass weeds in generated images. The generated images overlapping with grass weeds lose the realness, and the trained model reduces the detection rate.

I. Calculating the Coordinate to Place the First Pseudo Morning Glory

- An image is randomly selected from the 517 grass weed background images as shown in Figure 4 (a).
- The selected image is divided into a 64×64 pixel grid. By calculating the number of pixels that contain white pixels in each grid, we find a black-only grid. The coordinates (x_0, y_0) of the black-only grid cells are randomly selected to avoid overlap with the grass weed region (Figure 4 (b)).

II. Placing the First Morning Glory Image

- The first GAN image (Figure 5 (a)) is rotated by 0, 90, 180, or 270 [deg].

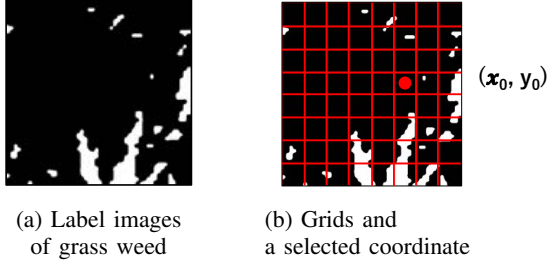


Fig. 4: Selection of coordinate to place the first pseudo image of morning glory (white area grass weed (weed), black: the others)

- Configuring a green bounding box of the morning glory region using OpenCV's `findContours` function `cv2.findContours()`
- Moving the green bounding box and the GAN image to the coordinates (x_0, y_0) obtained in Fig. 4 (b) (Figure 5 (b)). Placing them to the background images (Figure 4 (b)) as shown in Figure 5 (c).
- The blue bounding box is configured to enlarge by 20 pixels from all sides of the green bounding box instead of the green bounding box. Adjusting the size of this bounding box can control the density of the pseudo images of the morning glory.

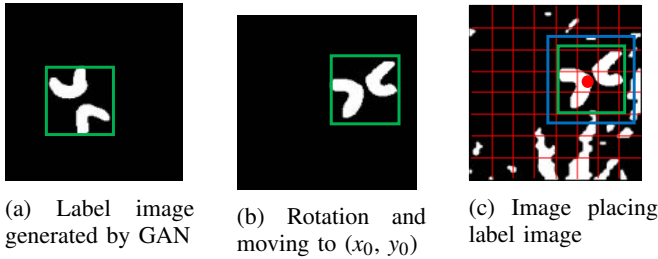


Fig. 5: Composition of GAN image of morning glory on grass weed background image (1st image)

III. Placing the Second and Subsequent Morning Glory Images.

- To express the naturalness of the density of morning glory in the image I , the locations of all plants should be configured. Based on the location of the first pseudo-morning glory, we define the area where to place the second and subsequent morning glory images. In the second and subsequent images, the distance to the grass weed (the white area) in the four directions (top, bottom, left, and right) is calculated from the coordinates calculated in the Fig 4 (b).
- For calculating the distance between the coordinate and the plants, we count the number of the grid that has no white pixels $N \in \{N_{\text{top}}, N_{\text{bottom}}, N_{\text{left}}, N_{\text{right}}\}$ as shown in Algorithm 1. By calculating the largest N , the area that has fewer plants is defined. The

pixel size of the grids is s .

Algorithm 1 Calculate the largest distance N

Require: $I \in (0, 1), x_0, y_0$

- 1: $\{N, N_{\text{top}}, N_{\text{bottom}}, N_{\text{left}}, N_{\text{right}}\} = 0$
- 2: $w = I.\text{width}(), h = I.\text{height}()$
- 3: **while** $0 \leq x_0 \pm i \cdot s, y_0 \pm i \cdot s \leq w, h$ **do**
- 4: **if** $\sum_{i=0}^h I(x_0, y_0 - i \cdot s) = 0$ **then**
- 5: $N_{\text{top}} = N_{\text{top}} + 1$
- 6: **if** $\sum_{i=0}^h I(x_0, y_0 + i \cdot s) = 0$ **then**
- 7: $N_{\text{bottom}} = N_{\text{bottom}} + 1$
- 8: **if** $\sum_{i=0}^w I(x_0 - i \cdot s, y_0) = 0$ **then**
- 9: $N_{\text{left}} = N_{\text{left}} + 1$
- 10: **if** $\sum_{i=0}^w I(x_0 + i \cdot s, y_0) = 0$ **then**
- 11: $N_{\text{right}} = N_{\text{right}} + 1$
- 12: **else**
- 13: **break**
- 14: $++i$
- 15: $N = \max N$
- 16: **return** N

- If there are no pixel values of 1 (white) in the grid, the function is iterated. The count numbers $N_{\text{top}}, N_{\text{bottom}}, N_{\text{left}}, N_{\text{right}}$ are incremented for each direction.
- Algorithm 1 is used to calculate the largest N in the four directions. The center position of the morning glory region in the second GAN image is composed with any edge of the blue bounding box in the direction with the largest N . Lines 4 to 5 show the algorithm that also finds N_{top} in the top direction, lines 6 to 7 show the algorithm that also finds N_{bottom} in the bottom direction, lines 8 to 9 show the algorithm that also finds N_{left} in the left direction and lines 10 to 11 show the algorithm that also finds N_{right} in the right direction. The I size of the image is 512. The width of the image is denoted as 'width' and the height as 'height'.
- For example, the left edge of the blue bounding box is selected because the distance in the left direction is the largest as shown in Figure 6. The second and subsequent GAN images are placed on the left edge as shown in Fig. 6 (a)). Figure 6 (b) is the RGB image generated by proposed placing.

B. SegNet

SegNet [15] is a type of semantic segmentation used to estimate images at the pixel level. It consists of an encoder that extracts features from the input image using a convolutional layer, and a decoder that maps the extracted features to their correspondence with pixel positions in the source image. We use SegNet to estimate the pixel of the morning glory using training data, including proposed pseudo-dense images.

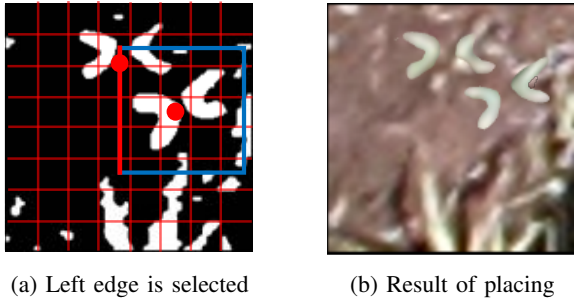


Fig. 6: Edge selection and result for placing the second GAN image

III. EXPERIMENTAL RESULT

A. Data Acquisition

In this research, the field images were acquired on 11 July 2022 from a growing season soybean field in Sabae, Fukui Prefecture, Japan. We used DJI Air 2S (Fig. 7) drone for capturing the field images, and the height capturing photos was 10 m from the ground. Sowing took place from 1 June 1 to 15 June 15 2022.



Fig. 7: DJI Air 2S ¹

B. Morning Glory Generation by PGGAN

PGGAN was used to generate morning glory images for pseudo-image creation. A total of 680 images with 90° rotation and vertical inversion data augmentation were used as training images for the 85 morning glory images obtained using the dataset collection method of Sumi et al [12]. Figure 8 shows input images of PGGAN in this research generated by the dataset collection method, which contains the various sizes from one field of the morning glory. The total iteration was set to 120,000 and the training was divided into four steps for each iteration: generating images with resolutions of 4×4 and 8×8, 16×16, 32×32 and 64×64, respectively. Learning is carried out in sequence, and a 64×64 image is finally generated.

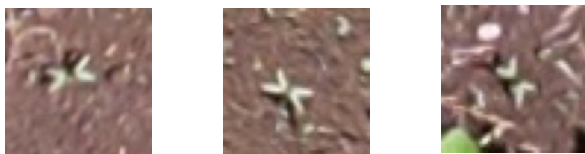


Fig. 8: GAN input images extracted by the dataset collection method [12]

Using PGGAN, the images generated at each step are shown in Figure 9. The image generated in step 4 of Fig. 9

is the final image, and it successfully generated an image similar to Fig. 1 (c). The size of the generated images is similar to the input images at the leaf age (Section III-A).

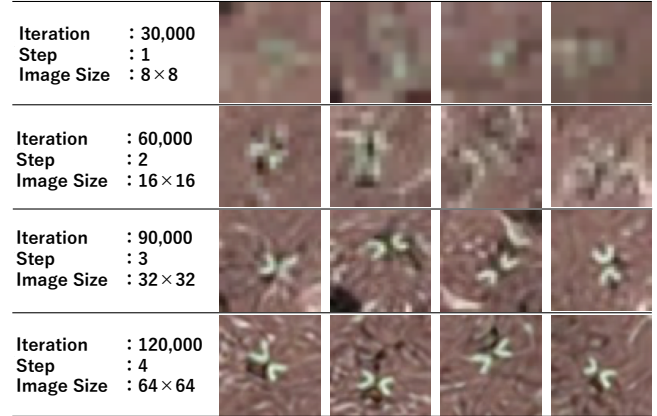


Fig. 9: Image generation result of morning glory by PGGAN

The generated pseudo morning glory data (Fig. 9 step 4) were labeled using α from Section III-D.1, with the morning glory regions estimated and used as the labeled images.

C. Image Generation of Pseudo-Dense Morning Glories

Region detection of grass weeds is implemented on 7848 cropped original aerial images, and 860 images are selected. In addition, soybean exclusion is implemented using ExG and 517 images are selected to be used as background images. Then, 300 morning glory images generated by PGGAN are used to generate pseudo-dense morning glory images.

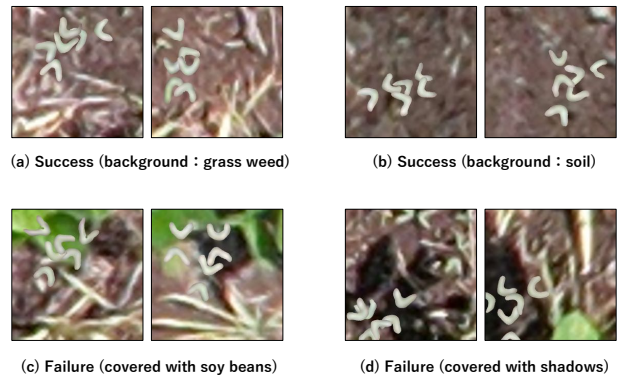


Fig. 10: Results of the image generation of pseudo-dense morning glories

Using the proposed image generation method, a successful image with grass weeds in the background is shown in Fig. 10 (a). A successful image with soil in the background is shown in Fig. 10 (b). A failed image covered with soybean is shown in Fig. 10 (c). A failed image covered with shadow is shown in Fig. 10 (d). Images that were placed into areas of soybean that could not be removed by ExG, or that were estimated to be negative by the grass weed model but

¹<https://www.dji.com/jp/support/product/air-2s>

were actually covered by shadows, resulting in unnatural composites, were considered as failed images.

Adjust the ratio between Fig. 10 (a) and (b), omitting the failed images and adding them to the dataset.

D. Estimation of morning glory

1) *Training without Generated Images of Pseudo-Dense Morning Glory using PGGAN (α)* : SegNet is used to learn the model to estimate the morning glory region. The model uses three classes for classification, which are morning glory, grass weeds, and the others (soil and soybeans). The morning glory and grass weed areas between the ridges in the drone image (5472×3648) are cropped to a size of 50×50 and used as one input image. Perform 90 [deg] rotation, vertical flipping, and contrast transformation on the 85 morning glory images obtained from trimming to expand the morning glory images to 1,360 images. Similarly, for 50 images of grass weeds, perform 90[deg] rotation and vertical flipping to expand them to 400 images. In addition, 400 images of soybean areas were cropped to a size of 50×50 pixels and added as another class, for a total of 2,160 images as training data. The input images are resized to 512×512 and divided 8:2 for training and validation. The kernel size is 5 and 100 epochs are used for training. The label image of the ground truth was manually annotated.

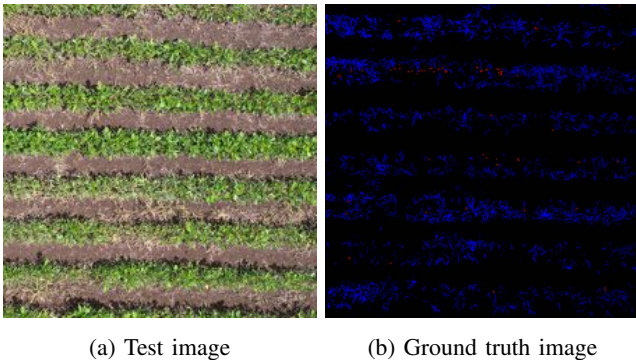


Fig. 11: Test image for estimation (red area: morning glory, blue area: grass weed, black: the others)

2) *Training with using Generated Images of Pseudo-Dense Morning Glory Created with PGGAN (β)* : As same as the configuration without GAN images in Section III-D.1, data augmentation on the cropped images was performed. We added 700 images of dense morning glory (Percentage of grass weeds used as background: 5%) to the 1,360 morning glory images, 100 grass weed images, and 400 soybean images, for a total of 2,560 images as training data. The input images were resized to 512×512 and divided 8:2 for training and validation. The kernel size was 5 and 200 epochs were used for training.

3) *Morning Glory Region Estimation using SegNet*: For estimation, a single aerial image cropped to 1800×1800 pixels was used. At the edges the image was distorted caused by the drone's camera lens, and we used cropped image for

evaluation. Additionally, due to resizing of the test images, estimation was performed on enlarged images resized by a factor of 10.24. The test image is shown in Fig. 11 (a). The ground truth image with manually annotated morning glory regions is shown in Fig. 11 (b). In this research, the focus was on whether data augmentation with PGGAN can enable the detection of dense morning glory without missing, so the Recall value was more important, and the F_2 score was selected.

E. Result of Estimation

TABLE I: Evaluation of the estimation of the morning glory region using pseudo-dense images of morning glory

	Recall	Precision	F_2 score
α : Not including pseudo images	0.279	0.415	0.299
β : Including pseudo images	0.402	0.411	0.404

The ground truth image with manual annotation is shown in Fig. 12 (a), the estimation results without adding the pseudo-image to the dataset are shown in Fig. 12 (b), and the estimation results with the pseudo-image added to the dataset are shown in Fig. 12 (c). The Recall, Precision, and F_2 score for each are presented in Table I calculated by using the morning glory data in the ground truth image as shown in Fig. 11 (b).

The enlarged images of the dense areas in Figs. 12 (a), (b) and (c) are shown in Figs. 13 (a), (b) and (c) respectively, and the estimated results of increasing the proportion of grass weeds used as background in the creation of pseudo-dense images from 5 % to 30 % are shown in Fig. 13 (d).

1) *Without Generated Images of Pseudo-Dense Morning Glory using PGGAN (α)* : As shown in Table I (α), Recall was 0.279, Precision was 0.415 and F_2 score was 0.299. Fig. 12 (b) shows that the area is well estimated for grass weeds. However, comparing Fig. 13 (a) and (b), the dense area of morning glory can hardly be estimated. It is not possible to estimate the morning glory in dense areas without pseudo-dense morning glory images.

2) *With Generated Images of Pseudo-Dense Morning Glory using PGGAN (β)* : As shown in Table I (β), Recall was 0.402, Precision was 0.411 and F_2 score was 0.404. Fig. 12 (c) shows that the estimated rate of grass weeds is decreasing. The estimated dense area of morning glory in Fig. 13 (c) shows an increase in the estimated area compared to Fig. 13 (b), although not as much as in Fig. 13 (a). As can be seen from the F_2 score values, the overall detection rate has increased. However, Precision has decreased. This may be due to the addition of complex representations such as 'dense areas of morning glory' and 'mixed areas of morning glory and grass weeds' during learning.

3) *30% of grass weeds used in the background*: Increasing the proportion of grass weeds in the background image from 5 % to 30 % mis-estimated morning glory as a grass weed because the proportion of grass weeds was too high. A small change in the proportion of grass weed images can significantly change the estimation results. Adjustment of the density proportion of morning glory and grass weeds is considered important.

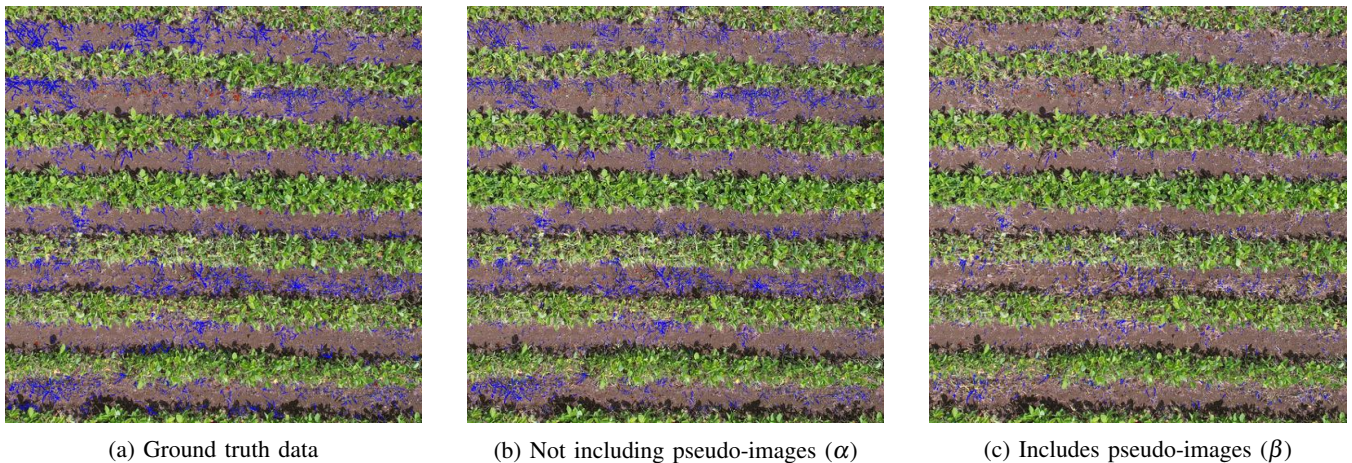


Fig. 12: Estimation results from SegNet using each dataset (red area : morning glory (weed), blue area : grass weeds (weed))

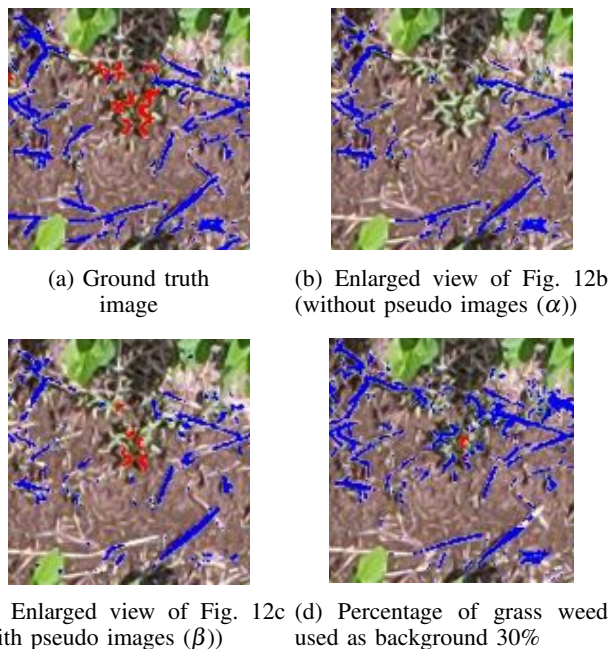


Fig. 13: Enlarged image of the dense area (red area: morning glory, blue area: grass weed)

IV. CONCLUSION

In this research, PGGAN was used to generate images of morning glories, which were then used to create pseudo-dense images of morning glories and mixed images of morning glories and grass weeds. By adding pseudo-images to the dataset, the trained model could classify species in dense areas, and the F_2 score was increased from 0.299 to 0.404.

In future works, we will implement to improve the algorithm for dense representation when creating pseudo-images and select background images of grass weeds to reduce the number of failed images as much as possible. We would also like to adjust the proportion of grass weeds and morning glories and improve the estimation model to make it easier

to estimate smaller targets. consider using a new model.

REFERENCES

- [1] Toshiyuki Monma et al. Smart agriculture and rural communities. *Journal of Rural Planning Association*, Vol. 40, pp. 134–137, 2021 (in Japanese).
- [2] Osorio Kavir et al. A deep learning approach for weed detection in lettuce crops using multispectral images. *AgriEngineering*, Vol. 2, No. 3, pp. 471–488, 2020.
- [3] J. Rasmussen et al. Pre-harvest weed mapping of *cirsium arvense* in wheat and barley with off-the-shelf uavs. *Precision Agriculture*, Vol. 20, pp. 983–999, 2019.
- [4] W Ramirez. Deep convolutional neural networks for weed detection in agricultural crops using optical aerial images. In *2020 IEEE Latin American GRSS & ISPRS Remote Sensing Conference (LAGIRS)*, pp. 133–137. IEEE, 2020.
- [5] Kamath Radhika et al. Classification of paddy crop and weeds using semantic segmentation. *Cogent engineering*, Vol. 9, No. 1, p. 2018791, 2022.
- [6] Hidenori Asami et al. Timely control of naturalised morning glory in multi-crop plots using the soybean leaf age progression model. *Weed research*, Vol. 66, pp. 1–10, 2021 (in Japanese).
- [7] Sadegh Mohajer et al. Effect of different herbicides on seed yield and physiological aspects in soybean (*glycine max l.*). *Recent Advances in Medicinal Plants and Their Cultivation*, Vol. 6, pp. 58–73, 2013.
- [8] LG Divyanth et al. Image-to-image translation-based data augmentation for improving crop/weed classification models for precision agriculture applications. *Algorithms*, Vol. 15, No. 11, p. 401, 2022.
- [9] Espejo-Garcia et al. Combining generative adversarial networks and agricultural transfer learning for weeds identification. *Biosystems Engineering*, Vol. 204, pp. 79–89, 2021.
- [10] Chen Dong et al. Synthetic data augmentation by diffusion probabilistic models to enhance weed recognition. *Computers and Electronics in Agriculture*, Vol. 216, p. 108517, 2024.
- [11] Ian Goodfellow et al. Generative adversarial nets. *Advances in neural information processing systems*, Vol. 27, , 2014.
- [12] Naoya Sumi et al. Automated detection of micro morning glory using aerial imagery in soybean fields-annotation based on vegetation index, shape, etc-. In *Robomech2023*, No. 2A2-A25, 2023 (in Japanese).
- [13] Tero Karras et al. Progressive growing of GANs for improved quality, stability, and variation. In *International Conference on Learning Representations*, 2018.
- [14] Woebbecke et al. Color indices for weed identification under various soil, residue, and lighting conditions. *Transactions of the ASAE*, Vol. 38, No. 1, pp. 259–269, 1995.
- [15] Badrinarayanan Vijay et al. Segnet: A deep convolutional encoder-decoder architecture for image segmentation. *IEEE Transactions on Pattern Analysis and Machine Intelligence*, Vol. 39, No. 12, pp. 2481–2495, 2017.